Electrical Power Quality and Utilisation, Journal Vol. XIV, No. 1, 2008

Effects of Source Voltage Harmonics on Power Factor Compensation in AC Chopper Circuits

M. Erhan BALCI, M. Hakan HOCAOGLU
Gebze Institute of Technology, Turkey

Summary: **In recent years, the detailed modelling of power electronic devices and their behaviours on various system conditions are a great concern of the power industries and customers. One of the widely proliferated such devices is the triac controlled ac choppers. Although these types of devices have important application areas, their poor power factor is the main obstacle for the large scale implementation in power systems. This paper presents an analysis on the behaviour of a single phase load composed with triac controlled ac chopper during the reactive power compensation with a basic capacitor in nonsinusoidal voltage case. The results of these analysis show that the distortion of voltage improves power factor, which is contradicting with previous findings, for the high conduction angles of triac controlled ac chopper. In addition, it is observed that the performance of power factor improvement with a basic capacitor is noticeably affected by the phase angles of voltage harmonics, which is an extensively ignored issue in the literature.**

Keywords:
harmonics,
ac chopper circuits,
power factor,
reactive power compensation,
nonsinusoidal condition

1. INTRODUCTION

For the systems, which are contaminated with nonsinusoidal voltages and currents, it is well known that power factor compensation and power definitions are the important issues and widely discussed in the literature [1-6]. The studies on power definitions can be divided into two groups; some of them are focused on physical meaning of power in nonsinusoidal conditions and correct interpretation of compensable power [1-4]. Others are specialized on the effects of harmonic distortion levels on reactive power compensation [5, 6]. In the studies, focused on physical meaning of power in nonsinusoidal conditions, conventional power definitions are analysed in nonsinusoidal condition by giving particular emphasis to the usefulness of active, reactive and distortion powers with the aims of not only exploration of the physical essence of the energy and power for the scientific consistency but also provision of engineering tools to achieve maximum power factor. All of these studies demonstrate that reactive power compensation is a challenging problem for power systems in nonsinusoidal conditions.

Single-phase loads composed with triac controlled ac chopper are frequently used power electronic loads in industrial applications; such as glass melting [7, 8], controlling of ac motor speed [9, 10] and dimming lamps [11]. In general, to achieve effective and proper operation, such applications come with a compensation problem to be solved in a cost efficient manner. The studies, that are presented in [7, 8], demonstrate a method for power factor improvement with proper filters for the glass melting industry applications of triac controlled ac chopper circuits. It is shown that significant improvement in the power factor can be achieved by filtering out the specific harmonics [7, 8]. The energy efficiency of triac controlled ac chopper circuits in the control of ac motor speed is the subject of the studies, which are presented in [9, 10]. The efficiency of ac motor is optimised by using ac chopper circuits. The study [11] experimentally analyses that phase-controlled dimmable electronic ballast for fluorescent lamps taking into account power factor correction and efficiency. In the studies [7-11], it is observed that the triac controlled ac chopper circuits are largely employed as an efficiency improvement tool and a cheap controller for ac motors, lamps and heaters although it has poor power factor due to its harmonic producing nature. Moreover, THD index, which is extensively used to characterize the compensation behaviour of these circuits, may not be a good indicator for the case of power factor of such devices owing to the fact that the angles of individual harmonics are omitted.

In this paper, a complete analytical model of a single phase load composed with triac controlled ac chopper is described taking into account the distortion and impedance of supply side [12]. The model, developed in this paper, is constructed by using differential state equations, which is applied on these type problems in some studies [13, 14]. Usage of a complete analytical model gives the opportunity to employ extensive parametrical analysis without causing computational burden, which may be present in the case of classical numeric computations [15-17] that are also used for this type of studies [18]. The model, developed in this paper, is used to investigate the effects of THD and harmonic phase angles of source voltage on power factor compensation with a basic capacitor, for various triac conduction angles. The effects on maximum power factor, which is available with a basic capacitor, and distortion factor, in the condition of maximum power factor, are thoroughly analyzed.

2. POWER FACTOR CHARACTERIZATION IN NONSINUSOIDAL CONDITIONS

In general, power factor is characterised as a function of total harmonic distortion of current (THD_I) or distortion factor (df) [4, 19-21]. In these characteristic analysis, power

factor (*pf*) is derived in harmonic domain by considering well known total harmonic distortion (*THD*) and distortion factor (*df*) indices as depicted in equation (1) and (2):

$$pf = \frac{P}{S} = \frac{P_1 + \sum_{n=2}^{\infty} P_n}{S_1 \cdot \sqrt{1+\left(THD_U/100\right)^2} \cdot \sqrt{1+\left(THD_I/100\right)^2}} \quad (1)$$

An appropriate estimation of power factor could also be determined by using equation (2) for low level voltage distortions:

$$pf \approx pf_{disp} \cdot \frac{1}{\sqrt{1+\left(THD_I/100\right)^2}} = pf_{disp} \cdot df \quad (2)$$

where distortion factor (*df*) and displacement power factor (pf_{disp}) determined as:

$$df = I_1/I, \; pf_{disp} = P_1/S_1 \quad (3)$$

On the other hand, in some studies on the triac controlled circuits, power factor is characterised as a function of conduction angle (α) [4, 22]. Power factor formula is derived by the process:
Determining the rms value of current:

$$I = \sqrt{\frac{1}{2\pi} \cdot \left[\int_{\alpha}^{\pi} i\left(\omega t\right)^2 d\omega t + \int_{\pi+\alpha}^{2\pi} i\left(\omega t\right)^2 d\omega t \right]} \quad (4)$$

where the current is $i\left(\omega t\right) = \frac{Um}{R_{Load}} Sin\left(\omega t\right)$ due to resistive load.
Consequently, the rms value of current can be defined as:

$$I = \frac{Um}{\sqrt{2} R_{Load}} \cdot \sqrt{\frac{2\left(\pi - \alpha\right) + Sin\left(2\alpha\right)}{2\pi}} \quad (5)$$

Finally, the power factor is formulised as in equation (7) by substituting equation (5) in equation (6):

$$pf = \frac{P}{S} = \frac{I^2 R_{Load}}{UI} \quad (6)$$

$$pf = \sqrt{\frac{2\left(\pi - \alpha\right) + Sin2\alpha}{2\pi}} \quad (7)$$

Due to the fact that source distortion is not considered in the analysis, these characteristic formulations may not be accurate enough to predict the characteristic of power factor and reactive power compensation of the triac controlled ac chopper circuit in the conditions, where source side distortion is considerably high and/or a line impedance is present. Moreover, THD of voltage and current may not be a good indicator for the characterisation of power factor compensation owing to the fact that the phase angles of current and voltage harmonics are not considered in THD indices. Thus, the effects of harmonic phase angles are not properly accounted. In this paper, the effects of these two parameters will be analysed thoroughly.

3. ANALYTICAL MODEL OF TRIAC CONTROLLED AC CHOPPER CIRCUIT

The system, given in Figure 1, has a triac controlled ac chopper circuit, a distribution line, a load, which is modelled as constant impedance, and a compensation capacitor, which is placed on the load terminal.

The system can be analyzed into two operating modes as triac conduction and triac cut off. During triac cut off mode, current and voltages are calculated by using super position theorem. During triac conduction mode, equations of current and voltage in the circuit are found by solving the system of equations given below:

$$u_s(t) = \sum_{n=1}^{n_{max}} Um_n \cdot Sin\left(\omega_n t + \varphi_n\right) \quad (8)$$

$$R_{Line} \cdot i_{Line}(t) + L_{Line} \cdot \frac{di_{Line}}{dt} + u_{Load}(t) = u_S(t) \quad (9)$$

$$R_{Load} \cdot i_{Load}(t) + L_{Load} \cdot \frac{di_{Load}}{dt} - u_{Load}(t) = 0 \quad (10)$$

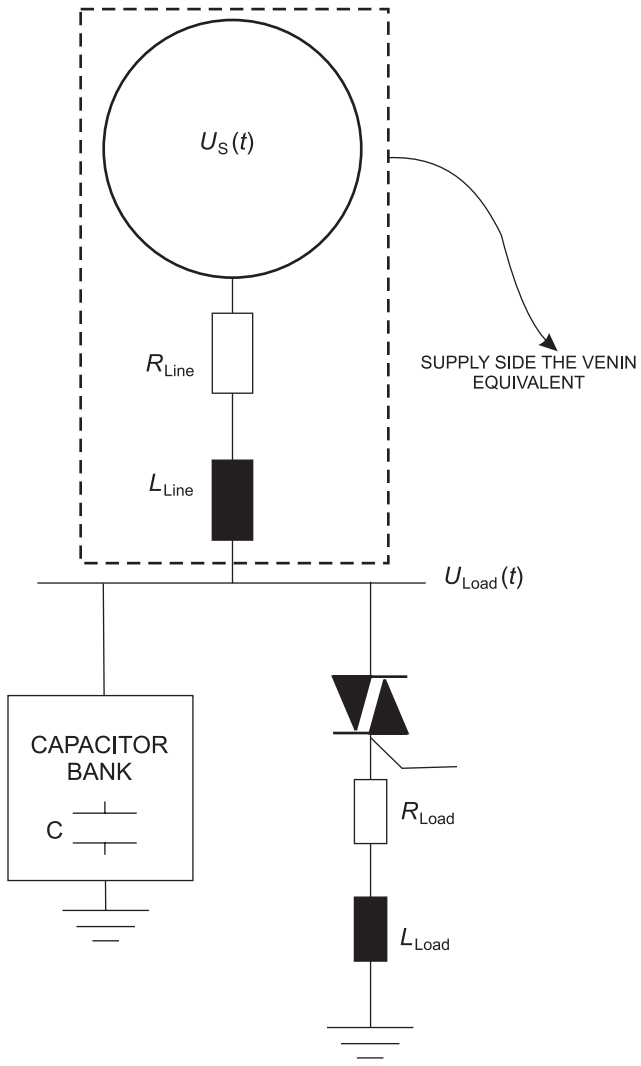

Fig. 1. Test system

$$i_{Line}(t) - i_{Load}(t) - C \cdot \frac{du_{Load}}{dt} = 0 \tag{11}$$

Equations (8–11) are solved for the initial conditions of line current, load voltage and load current. The solution of the system for line current $i_{Line}(t)$, load voltage $u_{Load}(t)$ and load current $i_{Load}(t)$ is:

$$i_{Line}(t) = \sum_{n=1}^{n_{max}} \left[A_n \cdot Sin(\omega_n \cdot t + \varphi_n) + B_n \cdot Cos(\omega_n \cdot t + \varphi_n) \right] + \\ + \sum_{n=1}^{n_{max}} \sum_{k=1}^{3} \left[ck_n \cdot e^{Dk \cdot t} \right] \tag{12}$$

$$u_{Load}(t) = \left\{ \sum_{n=1}^{n_{max}} \left[(Um_n - R_{Line} \cdot A_n + L_{Line} \cdot B_n \cdot \omega_n) \cdot Sin(\omega_n \cdot t + \varphi_n) \right] + \right. \\ + \sum_{n=1}^{n_{max}} \left[(-R_{Line} \cdot B_n - L_{Line} \cdot A_n \cdot \omega_n) \cdot Cos(\omega_n \cdot t + \varphi_n) \right] - \\ \left. - \sum_{n=1}^{n_{max}} \sum_{k=1}^{3} \left[(R_{Line} + L_{Line} \cdot D_k) \cdot ck_n \cdot e^{D_k \cdot t} \right] \right\} \tag{13}$$

$$i_{Load}(t) = \left\{ \sum_{n=1}^{n_{max}} \left[(A_n - C \cdot R_{Line} \cdot B_n \cdot w_n - C \cdot L_{Line} \cdot A_n \cdot w_n^2) \cdot Sin(w_n \cdot t + \varphi_n) \right] + \right. \\ + \sum_{n=1}^{n_{max}} \left[(B_n - Um_n \cdot C \cdot \omega_n + R_{Line} \cdot A_n \cdot C \cdot \omega_n - L_{Line} \cdot B_n \cdot C \cdot \omega_n^2) \cdot Cos(\omega_n \cdot t + \varphi_n) \right] + \\ \left. + \sum_{n=1}^{n_{max}} \sum_{k=1}^{3} \left[(1 + R_{Line} \cdot C \cdot D_k + L_{Line} \cdot C \cdot D_k^2) \cdot ck_n \cdot e^{D_k \cdot t} \right] \right\} \tag{14}$$

where A_n, B_n and ck_n are the coefficients for n^{th} harmonic of the source voltage. These coefficients and initial values of line current, load voltage and load current are given in Appendix. Triac cut-off time $t_{cut\text{-}off}$ is the solution of the following equation:

$$i_{Load}\left(t_{cut-off}\right) = 0 \tag{15}$$

for interval $t_{conduction} < t_{cut\text{-}off} < (t_{conduction} + T_f/2)$. Solution for the sinusoidal voltage source and nonlinear load case could easily be obtained by substituting $n = 1$ in the equations from (8) to (15).

In order to demonstrate accuracy of the solutions the results obtained by this method compared with the results produced by ATP version of EMTP [15] for 90˚ triac conduction angle, as depicted in Figure 2.

The analytical computation and EMTP results are in very close agreement.

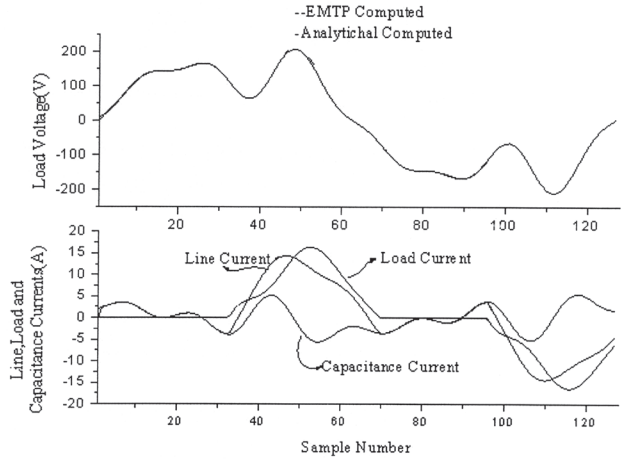

Fig. 2. Comparison of the results of analytical model and EMTP in time domain

4. ANALYSIS

To show the effects of total harmonic distortion and harmonic's phase angles of source voltage over the reactive power compensation with a basic capacitor, maximum power factor and distortion factor, in the condition of maximum power factor, are calculated by using proposed analytical model for the various cases of triac conduction angles and source voltage's distortion. Two different parametrical analyses are considered in the system. In the first case, maximum power factor and current distortion factor, in the condition of maximum power factor, are calculated for various triac conduction angles between 45˚ and 135˚. In each case of triac conduction angles, the THD_U of source voltage is varied from 1% to 14%. In the second case, the effects of source voltage's harmonic phase angles on the maximum power factor, available with a basic capacitor, and current distortion factor, in the condition of maximum power factor, are analysed by varying the harmonic phase angles of source voltage when source voltage's total harmonic distortion (THD_U) is 10%.

Case 1

In this case, the effect of THD_U on reactive power compensation, power factor and distortion factor are analysed in the systems with triac controlled ac chopper loads. The RMS value of source voltage is kept constant while adjusting the magnitudes of harmonic voltages namely 3rd, 5th, 7th harmonics of fundamentals. Source voltage waveforms and harmonic magnitudes at 1% and 14% of THD_U are given in Figure 3.

For various values of THD_U and triac half cycle conduction angle, the curves of maximum power factor, available with a basic capacitor, are shown in Figure 4.

It is clear from Figure 4 that maximum power factor is decreased by THD_U in the triac half cycle conduction angle interval from 45˚ to 90˚. For 45˚, maximum power factor is varied from 0.96 to 0.88 in the interval of THD_U from 1% to 14%. In the cases of 55˚ and 65˚, the slope of maximum power factor curve is the same as in the case of 45˚. It is interesting to observe that maximum power factor is increased by THDU in triac half cycle conduction angle interval from 110˚ to 135˚. The slope of maximum power

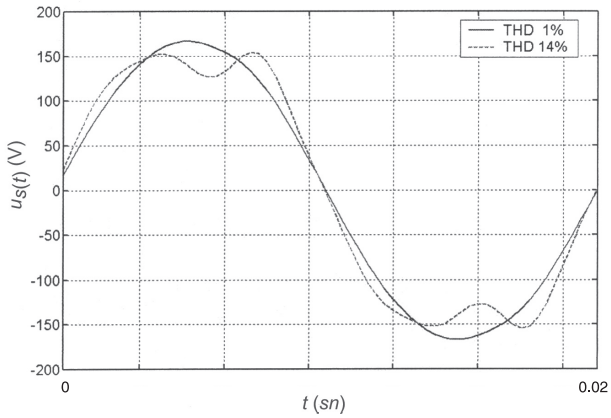

Fig. 3a. Source voltage waveforms for the 1% and 14% values of THD_u

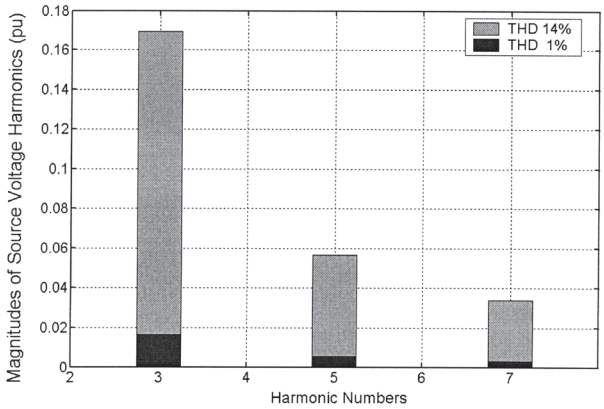

Fig. 3b. Source voltage's harmonic spectrums for the 1% and 14% values of THD_u

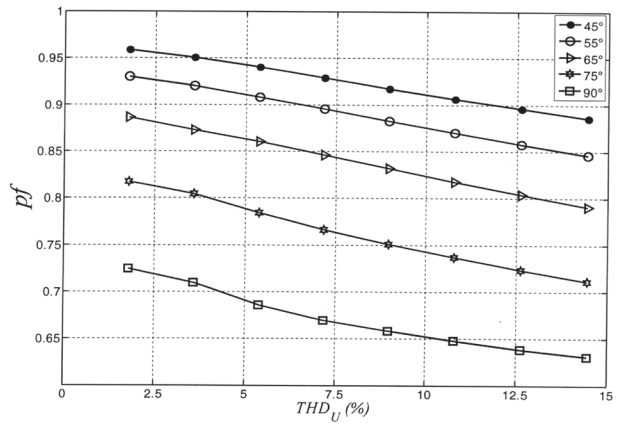

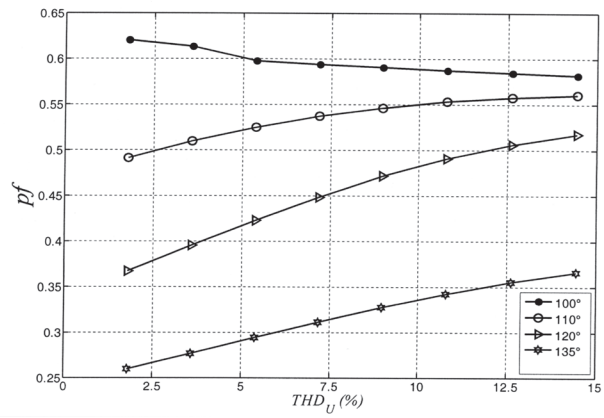

Fig. 4. Maximum power factors, available with a basic capacitor, for various values of THD_U and triac half cycle conduction angles

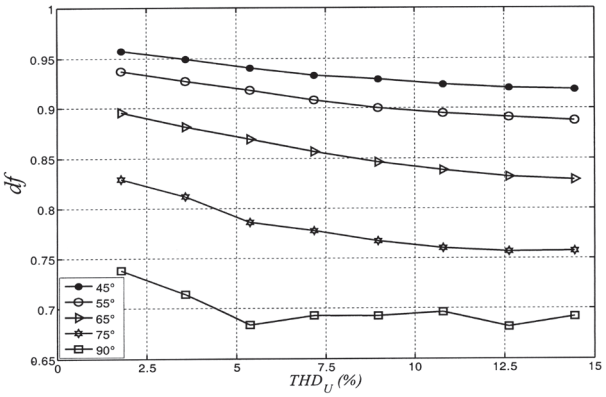

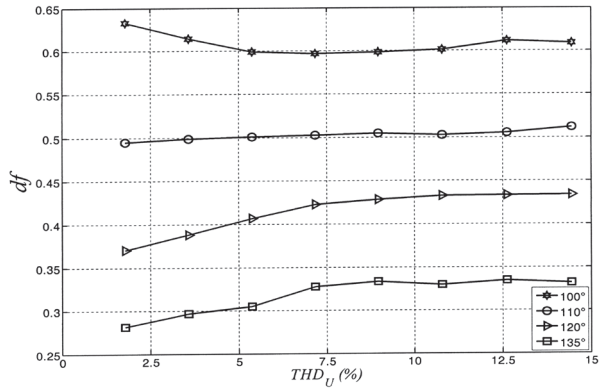

Fig. 5. Variation of *df*, in the condition of maximum power factor, for various values of THD_U and triac half cycle conduction angles

factor curve, for 120˚, is more significant than the slopes of the curves for 110˚ and 135˚.

For the same case, the curves of current distortion factor, in the condition of maximum power factor, are shown in Figure 5.

Due to the fact that line current's harmonics, generated by the load, are in the same directions with source voltage's harmonics in triac half cycle conduction angle interval from 45˚ to 75˚, current distortion factor is decreased by THD_U. For 120˚ and 135˚, distortion factor is increased by THD_U owing to the fact that line current's harmonics, generated by load side, and source voltage's harmonics are in the opposite direction. On the other hand, the trends of current distortion factor, for 90˚ and 100˚, demonstrate irregularities by the variation of THD_U.

Case 2

In order to quantify the effect of harmonic phase angles of source voltage on reactive power compensation, the harmonic phase angles of source voltage are varied according to equation 16 with keeping the phase angle of source voltage's fundamental harmonic as constant (φ_1=0˚).

$$\varphi_n = n\ \delta \tag{16}$$

It is shown from Figure 6 that different waveforms might appear in the power systems for the same THD_U. Consequently, the variation of maximum power factor and current distortion factor, in the condition of maximum power factor, must be analyzed to define the characteristic

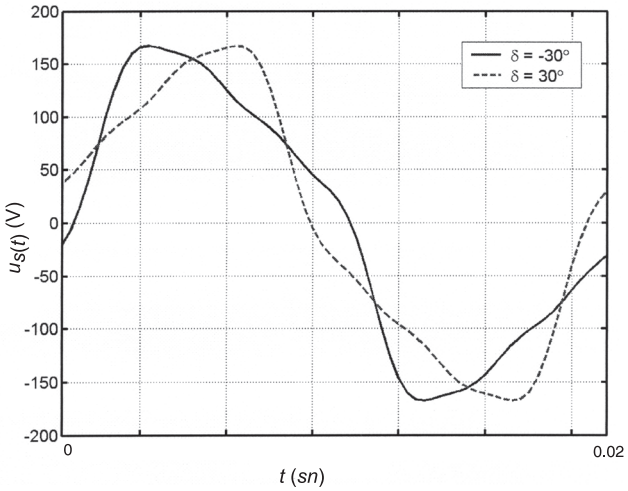

Fig. 6. Source voltage waveforms of δ = -30˚ and δ = 30˚ cases for THD_U = 10%

of reactive power compensation of the circuit in the cases of nonsinusoidal source voltage.

For various values of source voltage's harmonic phase angles and triac half cycle conduction angles, the curves of maximum power factor, available with a basic capacitor, are shown in Figure 7.

For 45˚ and 55˚ values of half cycle conduction angle, the curves of maximum power factor, available with a basic capacitor, are minimum in the case of voltage's harmonic phase angles around $\delta = -15^{\circ}$. On the other hand, for 90˚, 120˚ and 135˚ values of half cycle conduction angle, maximum power factor curves make a peak in the interval between 10˚ and 25˚ of δ. In spite of the trends, which are apparent for 45˚, 55˚, 90˚, 120˚ and 135˚ values of half cycle conduction angle, the general trend of maximum power factor curves is almost linear in other conduction angles.

For the same case, the curves of current distortion factor, in the condition of maximum power factor, are shown in Figure 8.

It is shown from Figure 8 that, for 135˚ value of triac half cycle conduction angle, the curve of current distortion factor demonstrates noticable irregularity in the variation interval of δ. For the triac conduction angles without 75˚ and 110˚, the curves of current distortion factor are minimum in the interval between –5˚ and 5˚ of δ. On the other hand, for the half cycle conduction angles without 135˚, the curves of current distortion factor demonstrate similar trend by the variation of δ.

5. CONCLUSION

In this paper, a complete analytical model of a single phase load composed with triac controlled ac chopper is utilized taking into account the distortion and impedance of voltage source to analyse its compensation characteristic.

The results show that, for high conduction angles, the distortion of source voltage improves the power factor, which is contradicting with the previous qualitative analysis about

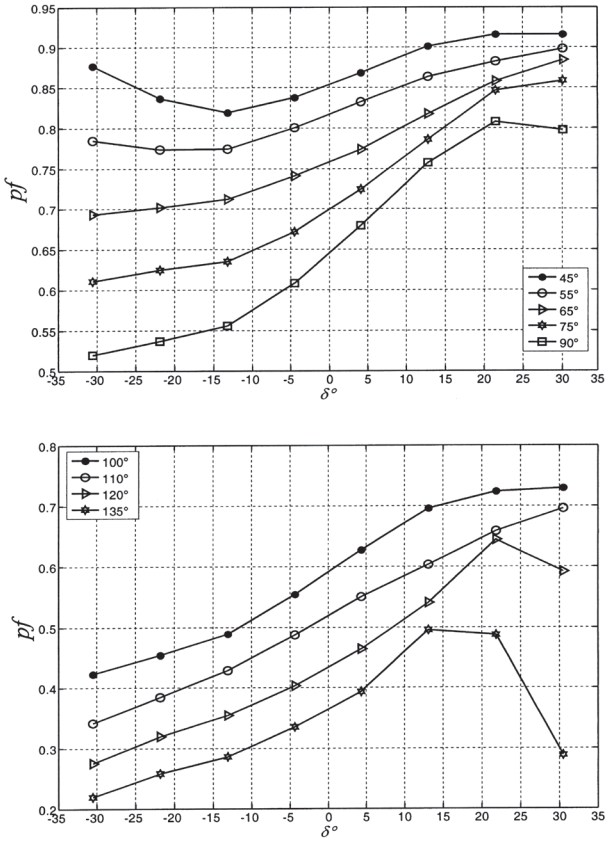

Fig. 7. Maximum power factors, available with a basic capacitor, for various values of δ (related to source voltage's harmonic phase angles) and triac half cycle conduction angles

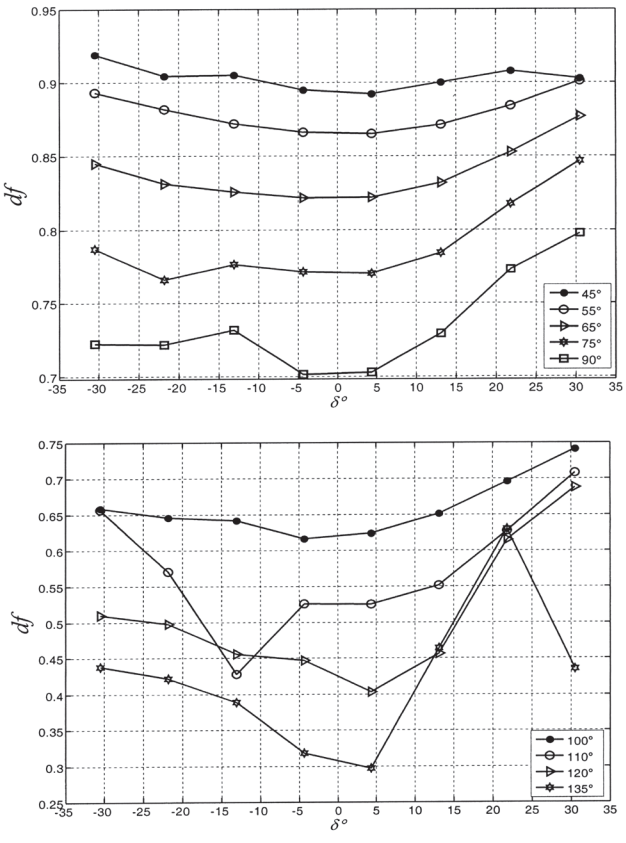

Fig. 8. Variation of *df*, in the condition of maximum power factor, for various values of δ (related to source voltage's harmonic phase angles) and triac half cycle conduction angles

the effects of source voltage's distortion over power factor. In the same THD_U values of source voltage, the phase angles of source voltage's harmonics are an important factor on power factor compensation and should be taken into account on their compensation characteristic. It could be concluded that THD indices and conduction angle are not enough to characterize power factor compensation process in the nonlinear circuits such as triac controlled ac chopper circuit.

As a result, source voltage harmonic's phase angles are an important indicator for the proper characterisation of harmonically contaminated circuits, such as ac chopper. Therefore, it should be incorporated with the harmonic distortion indices. This will be considered as a future work.

The List of Symbols:

$THD_{U,I}$ — Total harmonic distortion of voltage or current
Um — Maximum value of source voltage
ω — Angular frequency
t — Time
U — Total RMS value of source voltage
I — Total RMS value of load current
I_1 — RMS value of load fundamental harmonic current
df — Current distortion factor
pf — Power factor
pf_{disp} — Displacement power factor
P_1 — Active power of fundamental harmonic
S_1 — Apparent power of fundamental harmonic
P_n — Active power of n^{th} harmonic
P — Active power
S — Apparent power
α — Triac conduction angle for first cycle in ac chopper circuit
Um_n — Maximum value of n^{th} harmonic in source voltage
φ_n — Source voltage phase angle of n^{th}
ω_n — Angular frequency of n^{th} harmonic
$u_s(t)$ — Source voltage
$i_{Load}(t)$ — Load current
$i_{Line}(t)$ — Line current
R_{Line} — Line Resistance
L_{Line} — Line inductance
R_{Load} — Load resistance
L_{Load} — Load inductance
C — Compensation Capacity
$t_{cut\text{-}off}$ — Triac cut-off time
$t_{conduction}$ — Triac conduction time for first cycle
T_f — Period of fundamental harmonic.

REFERENCES

1. Emanuel A.E.: *Powers in nonsinusoidal situations-a review of definitions and physical meaning*. IEEE Transactions on Power Delivery 1990; 3:1377–1389.
2. Czarnecki L.S.: *Comparison of power definitions for circuits with nonsinusoidal waveforms*. IEEE Tutorial Course 90EH0327-7-PWR 1990; 43–50.
3. IEEE Standard 1459–2000: *IEEE trial-use standard definitions for the measurement of electric power quantities under sinusoidal, nonsinusoidal, balanced, or unbalanced conditions.* IEEE Press.
4. Shepherd W., Zand P.: *Energy flow and power factor in nonsinusoidal circuits*. 1st edn, Cambridge University Press: Cambridge, 1979.
5. Raonic D., Cyganski D., Emanuel A.E.: *Power factor compensation at buses with slightly distorted voltage due to random harmonics.* IEEE Transactions on Power Delivery 1989; 1: 502–507.
6. Sasdelli R., Montanari G.C.: *Compensable power for electrical systems in nonsinusoidal conditions.* IEEE Transactions on Instrumentation and Measurement 1994; 4:592 – 598.
7. Sueker K.H., Hummel S.D., Argent R.D.: *Power factor correction and harmonic mitigation in a thyristor controlled glass melter.* IEEE Transactions on Industry Applications 1989; 6: 972–975.
8. Mendis S.R., Gilker C., Casarez C.: *Power factor and harmonic analysis of a modern glass fiber manufacturing plant.* Industry Applications Society Annual Meeting 1990, 1959–1964.
9. Benbouzid M.E.H., Beguenane R., Dessoude M., Hubbi W.: *Energy optimized control strategy for a variable input voltage three-phase induction motor*. IEEE International Electric Machines and Drives Conference Record 1997; MD2/5.1 – MD2/5.3.
10. Tomita H., Haneyoshi T., Miyashita O., Maeda A.: *An optimal efficiency control for energy saving of ac motor by thyristor voltage controller.* IECON '88 14 Annual Conference of Proceedings 1988; 3:816–819.
11. Wing-Hung Ki, Jiying Shi, Elson Yau, Mok P.K.T., Sin J.K.O.: *Phase-controlled dimmable electronic ballast for fluorescent lamps*. IEEE 30th Annual Power Electronics Specialists Conference 1999; 2: 1121–1125.
12. Balci M.E., Hocaoglu M.H.: *Comparison of power definitions for reactive power compensation in nonsinusoidal conditions.* IEEE Proceeding of 11th ICHQP 2004; 519–524.
13. Mansoor A., Grady W.M., Thallam R.S., Doyle M.T., Krein S.D., Samotyj M.J.: *Effect of supply voltage harmonics on the input current of single-phase diode bridge rectifier loads*. IEEE Transactions on Power Delivery 1995; 3: 1416–1422.
14. Carpinelli G., Iacovone F., Russo A., Varilone P., Verde P.: *Analytical modeling for harmonic analysis of line current of VSI-fed drives.* IEEE Transactions on Power Delivery 2004; 3: 1212–1224.
15. CAN/AM EMTP User Group. Alternative Transient Program (ATP) Rule Book. (Canadian/American EMTP User Group, 1992).
16. MicroSim Corporation. PSpice Reference Manual, 1991.
17. Math Works Inc., Notes of SimPowerSystems 4.1., (Online) http://www.mathworks.com/products/simpower.
18. Rajagopalan V.: *Modeling and simulation of power electronic converters for power supplies*. IEEE Proceedings of 21st IECON 1995. 1: 27–32.
19. Grady W.M., Gilleskie R.J.: *Harmonics how they relate to power factor*. EPRI Proceeding of the Power Quality Issues & Oppertunities Conference 1993.
20. Marafao F.P., Deckmann S.M., Marafao J.A.G.: *Power factor analysis under nonsinusoidal and unbalanced systems.* IEEE proceeding 10th ICHQP 2002; 1: 266–271.
21. Mitchell J.E.: *Distortion factor: the `new' problem of power factor.* 14th International Telecommunications Energy Conference 1992; 514–516.
22. Hua J.: *Low voltage dimming system*. Industry Applications Conference 34th IAS Annual Meeting 1999, 3: 1700–1704.

APPENDIX:

$$A_n = \frac{\begin{vmatrix} \Delta_{1,n} & \Delta_{5,n} \\ \Delta_{2,n} & \Delta_{6,n} \end{vmatrix}}{\begin{vmatrix} \Delta_{3,n} & \Delta_{5,n} \\ \Delta_{4,n} & \Delta_{6,n} \end{vmatrix}}, \quad B_n = \frac{\begin{vmatrix} \Delta_{3,n} & \Delta_{1,n} \\ \Delta_{4,n} & \Delta_{2,n} \end{vmatrix}}{\begin{vmatrix} \Delta_{3,n} & \Delta_{5,n} \\ \Delta_{4,n} & \Delta_{6,n} \end{vmatrix}}$$

where:

$$\Delta_{1,n} = L_{Load} \cdot C \cdot Um_n \cdot w_n^2 - Um_n \qquad \Delta_{2,n} = -R_{Load}\, C Um_n\, w_n$$

$$\Delta_{3,n} = (R_{Line} \cdot L_{Load} \cdot C + R_{Load} \cdot L_{Line} \cdot C) \cdot w_n^2 - R_{Load} - R_{Line}$$

$$\Delta_{4,n} = L_{Load} \cdot L_{Line} \cdot C \cdot w_n^3 - (R_{Load} \cdot R_{Line} \cdot C + L_{Line} + L_{Load}) \cdot w_n$$

$$\Delta_{5,n} = -L_{Load} \cdot L_{Line} \cdot C \cdot w_n^3 + (R_{Load} \cdot R_{Line} \cdot C + L_{Line} + L_{Load}) \cdot w_n$$

$$\Delta_{6,n} = (R_{Line} \cdot L_{Load} \cdot C + R_{Load} \cdot L_{Line} \cdot C) \cdot w_n^2 - R_{Load} - R_{Line}$$

$$c1_n = \frac{\begin{vmatrix} \varepsilon_{1,n} & \delta_{2,n} & \delta_{3,n} \\ \varepsilon_{2,n} & \lambda_{2,n} & \lambda_{3,n} \\ \varepsilon_{3,n} & \gamma_{2,n} & \gamma_{3,n} \end{vmatrix}}{\begin{vmatrix} \delta_{1,n} & \delta_{2,n} & \delta_{3,n} \\ \lambda_{1,n} & \lambda_{2,n} & \lambda_{3,n} \\ \gamma_{1,n} & \gamma_{2,n} & \gamma_{3,n} \end{vmatrix}} \qquad c2_n = \frac{\begin{vmatrix} \delta_{1,n} & \varepsilon_{1,n} & \delta_{3,n} \\ \lambda_{1,n} & \varepsilon_{2,n} & \lambda_{3,n} \\ \gamma_{1,n} & \varepsilon_{3,n} & \gamma_{3,n} \end{vmatrix}}{\begin{vmatrix} \delta_{1,n} & \delta_{2,n} & \delta_{3,n} \\ \lambda_{1,n} & \lambda_{2,n} & \lambda_{3,n} \\ \gamma_{1,n} & \gamma_{2,n} & \gamma_{3,n} \end{vmatrix}}$$

$$c3_n = \frac{\begin{vmatrix} \delta_{1,n} & \delta_{2,n} & \varepsilon_{1,n} \\ \lambda_{1,n} & \lambda_{2,n} & \varepsilon_{2,n} \\ \gamma_{1,n} & \gamma_{2,n} & \varepsilon_{3,n} \end{vmatrix}}{\begin{vmatrix} \delta_{1,n} & \delta_{2,n} & \delta_{3,n} \\ \lambda_{1,n} & \lambda_{2,n} & \lambda_{3,n} \\ \gamma_{1,n} & \gamma_{2,n} & \gamma_{3,n} \end{vmatrix}}$$

where:

$$\varepsilon_{1,n} = i_{Line,n} - A_n \cdot sin(\omega_n \cdot t_i + \varphi_n) - B_n \cdot cos(\omega_n \cdot t_i + \varphi_n)$$

$$\varepsilon_{2,n} = \{u_{Load,n} - (Um_n - R_{Line} \cdot A_n + L_{Line} \cdot B_n \cdot \omega_n) \cdot sin(\omega_n \cdot t_i + \varphi_n) +$$

$$+ (R_{Line} \cdot B_n + L_{Line} \cdot A_n \cdot \omega_n) \cdot cos(\omega_n \cdot t_i + \varphi_n)\}$$

$$\varepsilon_{3,n} = \{-[A_n - \omega_n \cdot C \cdot (R_{Line} \cdot B_n + L_{Line} \cdot A_n \cdot \omega_n)] \cdot sin(\omega_n \cdot t_i + \varphi_n$$

$$+[-B_n + C \cdot \omega_n \cdot (Um_n - R_{Line} \cdot A_n + L_{Line} \cdot B_n \cdot \omega_n)] \cdot cos(\omega_n \cdot t_i +$$

$$\delta_{1,n} = e^{D_1 t_i},\ \delta_{2,n} = e^{D_2 t_i},\ \delta_{3,n} = e^{D_3 t_i}$$

$$\lambda_{1,n} = (-R_{Line} - L_{Line} \cdot D_1) \cdot e^{D_1 \cdot t_i}$$

$$\lambda_{2,n} = (-R_{Line} - L_{Line} \cdot D_2) \cdot e^{D_2 \cdot t_i}$$

$$\lambda_{3,n} = (-R_{Line} - L_{Line} \cdot D_3) \cdot e^{D_3 \cdot t_i}$$

$$\gamma_{1,n} = (1 + R_{Line} \cdot C \cdot D_1 + L_{Line} \cdot C \cdot D_1^2) \cdot e^{D_1 \cdot t_i}$$

$$\gamma_{2,n} = (1 + R_{Line} \cdot C \cdot D_2 + L_{Line} \cdot C \cdot D_2^2) \cdot e^{D_2 \cdot t_i}$$

$$\gamma_{3,n} = (1 + R_{Line} \cdot C \cdot D_3 + L_{Line} \cdot C \cdot D_3^2) \cdot e^{D_3 \cdot t_i}$$

and the initial values of line current and load voltage related to n^{th} harmonic of voltage source:

$$i_{Line,n} = \frac{Um_n \cdot sin(\omega_n t_i + \varphi_n - \phi_n)}{\left| R_{Line} + j\left(\omega_n L_{Line} - \frac{1}{\omega_n C} \right) \right|}$$

$$u_{Load,n} = -i_{Line,n} \cdot j \frac{1}{\omega_n C}$$

$$\phi_n = arctan\left(\frac{\left(\omega_n L_{Line} - \frac{1}{\omega_n C} \right)}{R_{Line}} \right)$$

($t_i = t_{conduction}$ for first cycle and $t_i = t_{conduction} + T_f/2$ for second cycle) Initial values of load current are zero at t_i for first and second cycle.

The characteristic equation is:

$$D^3 + \frac{\alpha_2}{\alpha_1} D^2 + \frac{\alpha_3}{\alpha_1} D + \frac{\alpha_4}{\alpha_1} = 0$$

where:

$$\alpha_1 = L_{Load} L_{Line} C$$

$$\alpha_2 = R_{Load} L_{Line} C + R_{Line} L_{Load} C$$

$$\alpha_3 = R_{Load} R_{Line} C + L_{Line} + L_{Load}$$

$$\alpha_4 = R_{Line} + R_{Load}$$

The roots of characteristic equation are:

$$D_1 = \frac{\beta}{6\alpha_1} - \frac{6\alpha_1\alpha_3 - 2\alpha_2^2}{3\alpha_1\beta} - \frac{\alpha_2}{3\alpha_1}$$

$$D_2 = -\frac{\beta}{12\alpha_1} + \frac{3\alpha_1\alpha_3 - \alpha_2^2}{3\alpha_1\beta} - \frac{\alpha_2}{3\alpha_1} + j\frac{\sqrt{3}}{2}\left(\frac{\beta}{6\alpha_1} + \frac{6\alpha_1\alpha_3 - 2\alpha_2^2}{3\alpha_1\beta} \right)$$

$$D_3 = -\frac{\beta}{12\alpha_1} + \frac{3\alpha_1\alpha_3 - \alpha_2^2}{3\alpha_1\beta} - \frac{\alpha_2}{3\alpha_1} - j\frac{\sqrt{3}}{2}\left(\frac{\beta}{6\alpha_1} + \frac{6\alpha_1\alpha_3 - 2\alpha_2^2}{3\alpha_1\beta} \right)$$

where:

$$\beta = \sqrt[3]{36\alpha_1\alpha_2\alpha_3 - 108\alpha_1^2\alpha_4 - 8\alpha_2^3 + 12\alpha_1 \cdot \sqrt{12\alpha_1\alpha_3^3 - 3\alpha_2^2\alpha_3^2 - 54\alpha_1\alpha_2\alpha_3\alpha_4 + 81\alpha_1^2\alpha_4^2 + 12\alpha_2^3\alpha_4}}$$

M. Hakan Hocaoglu
received the B.Sc. and M.Sc. degrees from Marmara University, Turkey. He obtained the Ph.D. degree in 1999 from Cardiff School of Engineering, UK. From 1988 to 1993, he worked at Gazinatep University, Turkey as a Lecturer. Since 1999, he has been with the Electronics Engineering Department of Gebze Institute of Technology, Turkey as an Assistant Professor. He is a member of IET.
Address:
Gebze Institute of Technology,
Department of Electronics Engineering,
Kocaeli, 41400, TURKEY
Tel.: (+90 262) 605 2440,
Fax: (+90 262) 653 84 90
E-mail: hocaoglu@gyte.edu.tr

M. Erhan Balci
received the B.Sc. degree from Kocaeli University and M.Sc. degree from Gebze Institute of Technology, Turkey. Since 2002, he has been with the Electronics Engineering Department of Gebze Institute of Technology, Turkey as an Research Assistant.
Address:
Gebze Institute of Technology,
Department of Electronics Engineering,
Kocaeli, 41400, TURKEY
Tel.: (+90 262) 605 2440,
Fax: (+90 262) 653 84 90
E-mail: m.balci@gyte.edu.tr